Fabricating hemocompatible bi-continuous PEGylated PVDF membranes via vapor-induced phase inversion

Antoine Venault, Jia-Ru Wu, Yung Chang, Pierre Aimar

Fabricating hemocompatible bi-continuous PEGylated PVDF membranes via vapor-induced phase inversion

Antoine Venault [a,*], Jia-Ru Wu [a], Yung Chang [a,b,**], Pierre Aimar [c]

[a] Department of Chemical Engineering, Chung Yuan Christian University, 200 Chung Pei Road, Chung-Li City 32023, Taiwan
[b] R&D Center for Membrane Technology, Chung Yuan Christian University, 200 Chung Pei Road, Chung-Li City 32023, Taiwan
[c] Laboratoire de Génie Chimique, Université Paul Sabatier, 118 Route de Narbonne, 31062 Toulouse Cedex 9, France

Keywords:
PEGylated PVDF membrane
VIPS process
Formation mechanisms
Antibiofouling
Hemocompatibility

A B S T R A C T

Lack of knowledge on their hemocompatibility limit the use of PVDF membranes in biomedical applications. Herein, we investigated the in situ modification of PVDF membranes by a PEGylated copolymer (PS_{60}-*b*-$PEGMA_{108}$) using vapor-induced phase separation (VIPS) process. Efforts were first oriented toward the characterization of the effect of copolymer on membrane formation, membranes physical properties and membranes surface chemistry. Then, biofouling was investigated before moving onto the hemocompatibility of membranes. Membranes structure tended to evolve from nodular to bi-continuous with PS_{60}-*b*-$PEGMA_{108}$ content, evidencing a change of dominating phenomena during phase inversion (crystallization-gelling vs. non-crystallization gelling), associated to a change of prevailing crystalline polymorph (β-polymorph vs. α-polymorph). Furthermore, the hydration of membranes was importantly enhanced, affecting nano-biofouling: bovine serum albumin, lysozyme and fibrinogen adsorption were drastically reduced, despite rough surfaces, highlighting the efficiency of the copolymer. Bacterial attachment tests revealed that macro-biofouling was inhibited as well. Results of erythrocytes, leukocytes, and thrombocytes adhesion indicated that membranes prepared from a casting solution containing 5 wt% copolymer are highly hemocompatible, result supported by low hemolysis ratio (1%) and delay of plasma clotting time. Overall, this study unveils that in situ modification coupled to the VIPS method can readily lead to hemocompatible PVDF membranes.

1. Introduction

The field of research on the design of hemocompatible materials for soft and hard organ replacements such as skin and bone has grown in importance over the past 15 years with breakthroughs in material science and biomedical engineering. Membrane scientists established that synthetic polymer membranes could play a key role too in biomedical engineering for the replacement of failing organs such as kidneys (dialysis) or lungs (blood oxygenators) provided that they are hemocompatible [1]. In general, all membranes intended to be used in biomedical applications meet similar requirements: they should resist biofouling due to body fluid proteins (e.g. plasma proteins), prevent the attachment of bacteria which could potentially lead to complications for patients, and not interact with blood cells. This tryptic must be considered regarding the important interplay between these species. Indeed, biofouling at a nano-scale (adhesion of proteins) can mediate fouling at a micro-scale (bacteria and cells) leading to undesired biological responses (biofilm formation, cell disruption) [2,3]. In addition, bacteria/cell can promote the adhesion of their alter egos through the establishment of hydrophobic–hydrophobic interactions. As several scales are considered, along with various natures of biologically interacting media, the development of ideal materials/membranes for blood treatment remains challenging.

Efforts can be oriented toward the modification of hydrophobic polymer membranes such as polysulfone, polyethersulfone or poly (vinylidene fluoride) (PVDF) as these polymers have proved in a number of commercial applications their outstanding resistances to mechanical, thermal or chemical stresses [4]. Meanwhile, their nature is a priori not favorable to a use in biomedical devices, as it is now acknowledged that hydrophobic materials tend to be more easily fouled than hydrophilic ones [5]. In this respect, a modification of these polymer membranes has to be undertaken. Many approaches exist, among which chemical surface modification processes, self-assembling methods or blending of polymers coupled to a phase inversion process (modification in situ) [6–10]. The latter one is regarded as potentially the easiest and the most

* Corresponding author. Tel.: +886 3 265 4113; fax: +886 3 265 4199.
** Corresponding author at: Department of Chemical Engineering, Chung Yuan Christian University, 200 Chung Pei Road, Chung-Li City 32023, Taiwan. Tel.: +886 3 265 4122; fax: +886 3 265 4199.
E-mail addresses: avenault@cycu.edu.tw (A. Venault), ychang@cycu.edu.tw (Y. Chang).

http://dx.doi.org/10.1016/j.memsci.2014.07.014

cost-effective method as it involves only one unit operation in the whole membrane preparation process, while the two first techniques aforementioned require to prepare the membrane and then to modify it. Surely, a number of issues arise such as the stability of the surface modification which is often questioned, or the effect of surface-modifying polymer on membrane formation mechanisms, but recent developments tend to show that they can be addressed. Indeed, by carefully designing the surface-modifier with respect to the intended application, optimum stability can be achieved. For instance, membranes aimed at being applied in water treatment should be modified with a water-insoluble amphiphilic copolymer possessing a strong anchoring block, as it has been done recently [11]. In addition, efforts must be made in the control of phase inversion kinetics in order to better tune membrane morphology, despite the presence of copolymer that can affect the mechanisms of membrane formation and as a result, its overall structuring [12]. The vapor-induced phase separation (VIPS) process involves slow mass transfer, compared to the popular wet-immersion process (also called liquid-induced phase separation), owing to the presence of the gas/liquid interface and the supplementary resistance to mass transfer arising from this interface. Hence, it may be an ideal process for a controlled preparation method of antibiofouling and hemocompatible membranes. Yet, nothing has been reported on this aspect, to the best of our knowledge.

In a series of recent works, we presented a novel block copolymer, polystyrene-*b*-poly(ethylene glycol) methacrylate (PS_m-*b*-$PEGMA_n$) along with its potential use for the design of antibiofouling membranes [11,13,14]. One of these copolymers was used to modify by dip-coating commercial PVDF membranes applied in membrane bioreactor for wastewater treatment, and antifouling properties along with stability of surface modification were shown to be excellent [14]. Indeed, PS blocks serve as anchoring blocks while PEGMA segments allow the formation of a hydration layer providing biofouling resistance. Moreover, as it is water-insoluble, long-term stability was expected, and was actually successfully demonstrated. Inspired from these previous studies, we have investigated the formation in one step of novel hemocompatible PVDF membranes by VIPS process, allowing not only the modification of the surface but also that of the deeper layers, as well as a better control of membrane formation mechanisms than traditional LIPS process. Casting solution was modified in situ before exposing it to water non-solvent vapors in controlled conditions of relative humidity and temperature. In this manuscript, we lay the focus on (i) membrane formation aspects through the analysis and the understanding of the effect of PS_m-*b*-$PEGMA_n$ on membrane structuring, (ii) biofouling at a nano- and macro-scale provided the strong relationship between biofouling and lack of hemocompatibility, and (iii) the effect of physicochemical parameters on the interactions between blood cells and membranes. We eventually aim at discussing the possibility of using PVDF membranes and these novel PEGylated PVDF membranes in blood filtration applications, because there is clearly a lack of knowledge on these aspects.

Table 1
Composition of casting solutions.

Membrane ID	PVDF (wt%)	PS_{60}-*b*-$PEGMA_{108}$ (wt%)	NMP (wt%)
Virgin PVDF	20	0	80
Mod-1	20	1	79
Mod-2	20	2	78
Mod-3	20	3	77
Mod-4	20	4	76
Mod-5	20	5	75

2. Experimental

2.1. Materials

Polyvinylidene fluoride (PVDF) granules (Mw = 150,000 g mol^{-1}) were bought from Kynar®, washed with methanol and deionized (DI) water, and dried under vacuum before use. PS_m-*b*-$PEGMA_n$ copolymer was synthesized following a method previously reported [13]. In the present work, it contains $m = 60$ repeat units polystyrene and $n = 108$ repeat units of poly(ethylene glycol) methacrylate. Its molecular weight and polydispersity index are 56,811 g mol^{-1} and 1.17, respectively, and were assessed by gas chromatography. 14 N-methylpyrrolidone (NMP) was the solvent used. It was purchased from Tedia and used directly without any purification step. DI water was obtained using a Millipore water purification system with a minimum resistivity of 18.0 MΩ cm.

2.2. Methods

2.2.1. Preparation of solutions

Solutions were prepared by blending PVDF and PS_{60}-*b*-$PEGMA_{108}$ copolymer in N-methylpyrrolidone at 32 °C. The choice of this particular copolymer (in terms of number of repeat units of each block) is mainly based on its compatibility with PVDF in NMP. Six solutions (total weight: 20 g) were prepared as presented in Table 1. Blends were continuously stirred for at least 24 h until obtaining homogeneous solutions. Degassing was performed for a few hours at ambient temperature and pressure, and solutions were allowed to rest until the use.

2.2.2. Preparation of membranes

Membranes were prepared by the VIPS process. Relative humidity (RH) and temperature in the chamber were set to 70% and 25 °C, respectively, one hour before casting the solutions in order to ensure thermodynamic equilibrium inside the chamber. Solutions were cast on glass slides using a metallic casting knife allowing controlling the initial thickness of the solutions to 300 μm. After exposing the polymeric system for 20 min to water vapors, glass slides were taken out of the chamber and gently immersed in a DI water bath for 24 h. Thereafter, newly formed membranes were pre-dried at ambient temperature directly on the glass slide on which they were prepared. Then, glass slides were immersed in water in order to separate membranes from their glass support, and membranes were finally dried on paper at ambient temperature. This two-step drying procedure permits to avoid potential shrinkage that often occurs when PVDF membranes are directly dried on paper after their formation by non-solvent induced phase separation.

2.2.3. Physicochemical characterization of membranes

Surface chemistry of membranes was investigated by performing Fourier Transform Infrared Spectrophotometry (FT-IR) and X-ray photoelectron spectroscopy (XPS) characterization. Instruments used as well as settings of parameters to perform characterization tests were similar to those reported earlier [14]. Therefore, one may want to refer to the literature for further details.

Structure of membranes was analyzed using scanning electron microscopy (SEM) and atomic force microscopy (AFM). For SEM characterization, membranes were mounted on a sample stage, sputter coated with gold for 150 s, and then introduced in the chamber of a Hitachi S-3000 instrument. Observations were performed setting the accelerating voltage to 5 keV or 7 keV, depending on the sample. For AFM studies in dry state, a JPK Instruments AG multimode NanoWizard (Germany) equipped

with a NanoWizard scanner was employed. The tip used was a commercial Si cantilever (TESP tip) of 320 kHz resonant frequency. Images were analyzed using JPK Image Processing software.

Tensile tests were carried out on a DMA 7e instrument (Perkin-Elmer) according to the ASTM D638-97 procedure. Samples (2 cm × 0.5 cm) were mounted between instrument clamps and tests carried out by gradually increasing the force at a rate of 250 mN/min, starting from 60 mN. Stress–strain plots were recorded on-line and analyzed using Merlin® software. 5 Measurements were performed for each membrane and the average of the values of the modulus of elasticity, tensile strength and elongation at break were taken as the mechanical properties of membranes.

Pore size of membranes was evaluated using a capillary flow porometer (CFP-1500-AXEL, PMI) according to a method previously described [15]. Porosity was assessed using ethanol (Aldrich). Preliminary tests permitted to ensure that there was no removal of PS_{60}-*b*-$PEGMA_{108}$ over the duration of the test. Dry membranes were weighed and subsequently immersed in ethanol for 24 h. After removing the excess of ethanol from the surface, wet membranes were weighed, and porosity assessed using the formula available in the literature [16,17].

2.2.4. Evaluation of hydration properties of membranes

Hydrophilicity of membranes was evaluated by measuring their surface water contact angle and their hydration capacity (mg/cm^3). Water contact angle was measured using an automatic contact angle meter (Kyowa Interface Science Co., Ltd. Japan) at 25 °C. DI water drop (4 μL) was deposited onto the surface of the membrane and contact angle measured after 3 s. 10 Measurements were performed for each membrane, and the average was taken as the final water contact angle of the membrane. Hydration capacity was evaluated using membrane disks of 1.3 cm diameter. After ensuring these disks were clean and dried, they were weighed, and then immersed in DI water for 24 h. Thereafter, superficial water was gently wiped out and wet membranes weighed. Hydration capacity was taken as the difference per unit porous volume between the wet weight and the dry weight. 5 Measurements were performed for each membrane and the average was taken as the final hydration capacity of the membrane.

2.2.5. Evaluation of protein adsorption and bacterial attachment onto membranes

Resistance to protein adsorption was evaluated using three different proteins: bovine serum albumin (BSA), lysozyme (LY) and fibrinogen (FN). BSA and LY adsorptions were tested at 25 °C according to a similar protocol, and described briefly as follows: each membrane disk (0.85 cm diameter) was placed in individual well of a 24-well plate. 1 mL of pure ethanol was poured onto the membranes to promote their swelling and diffusion of protein in next steps. After 30 min of immersion in alcohol, membranes were then soaked in phosphate-buffered saline (PBS) for 2 h. PBS was then removed and membranes were incubated with 1 mL of the desired protein (1 mg/mL) for 2 h. Concentration of protein remaining in the solution, and so amount of protein adsorbed by the membrane, was evaluated by measuring the absorbance of the solution at 280 nm using a UV–visible spectrophotometer (PowerWave XS, Biotech). Tests were performed three times on each membrane. As for FN adsorption, it was tested by the so-called ELISA test, which has been reported many times in the literature [18,19].

Resistance to bacterial attachment was performed using *Staphylococcus epidermidis* (SE) and *Escherichia coli* (EC). Methods related to the culture of bacteria were reported elsewhere [14]. PVDF and PEGylated membranes were incubated at 37 °C with *S. epidermidis* or *E. coli* suspension medium for 3 h. Membranes were then rinsed 9 times with DI water and dried under atmospheric pressure at room temperature (about 25 °C). Thereafter, membranes were contacted with Agar plates (Invitrogen) for 20 min. Membranes were then removed, and Agar plates shaken at 100 rpm for 8 h within an incubator inside which the temperature was maintained at 37 °C. Afterwards, the surface of Agar plates was observed and photographs taken with a Panasonic DMA-GF6 camera.

2.2.6. Evaluation of hemocompatibility of membranes

Hemocompatibility of membranes was assessed using a number of tests including erythrocytes, leukocytes and thrombocytes adhesion, hemolysis and blood clotting. Concerning red blood cells (RBCs) and white blood cells (WBCs) adhesion tests, cells were first isolated from other blood components. For RBCs, 250 mL of fresh blood obtained from a healthy human volunteer was centrifuged for 10 min at 1200 rpm to isolate the erythrocytes from the other blood components. Then 1 mL of the bottom layer containing erythrocytes was poured onto the membrane disks (0.4 cm^2) placed in a 24-well tissue culture plate and previously equilibrated for 24 h at 37 °C using 1 mL of PBS. Incubation of red blood cells with the membranes was carried out for 2 h at 37 °C. Membranes were then washed six times with 1 mL of PBS. Thereafter, they were soaked for 10 h into a 2.5% (v/v) glutaraldehyde solution in PBS maintained at 4 °C in order to fix the adhered erythrocytes. Membranes were then thoroughly washed five times with PBS. A Confocal microscope (LSCM, A1R, Nikon, Japan) was used to observe blood cells adhering onto the membranes' surface. Images were taken at λ_{ex}=488 nm/λ_{em}=520 nm, in *z*-steps of 1 μm, at three different places on the same chip and at a 200 × magnification. A similar procedure was used for WBCs. 250 mL of human blood was centrifuged at 500 rcf for 30 min. The intermediate phase between the top layer (platelets) and the bottom one (red blood cells) was constituted of WBCs. V=1 mL of white blood cells concentrate was poured onto clean and equilibrated membranes, and incubation performed for 120 min. After a post-treatment similar to that used for RBCs, surfaces were observed using a confocal microscope, following the exact same procedure as that used to study the adhesion of RBCs. As for thrombocytes adhesion, platelet-rich plasma (PRP) was obtained after centrifugation of 250 mL of fresh blood at 1200 rpm for 10 min. After separation of PRP from the other blood constituents, final thrombocytes concentration was evaluated to be about 10^5 cells/mL. Membranes were placed in a tissue culture plate, and each well was equilibrated with phosphate buffered solution (PBS), for 2 h at 25 °C. PBS was removed and 200 μL of PRP poured onto the membrane disks. After 2 h incubation at 37 °C, membranes were rinsed with 1 mL of PBS, steps were repeated six times, before being immersed into a PBS solution containing 2.5% (v/v) glutaraldehyde of PBS. These steps were run at 4 °C overnight, and aimed to fix the adhered platelets along with the adsorbed proteins onto the surface of the membranes. Surfaces were then observed using a confocal microscope with the same settings as those used for the observation of erythrocytes and leukocytes.

RBC hemolysis test was conducted according to the following protocol. After isolating RBCs by centrifugation, cells were washed three times using a saline solution (0.15 M). Clean and dried membranes (0.4 cm^2) were placed into a 24-well plate, and incubated with 500 μL of RBCs in PBS (corresponding to about 10^8 RBCs) at 37 °C and for 60 min. Then, solutions in contact with the membrane were centrifuged for 5 min at 2000 rpm in order to separate intact RBCs from disrupted cells. Absorbance of supernatants was measured at 541 nm (PowerWave spectrophotometer). 100% Lysis was obtained with DI water (positive control) while almost 0% lysis (negative control) was obtained with PBS. Tests

were repeated 6 times for each membrane and the average reported as the final hemolysis ratio.

The clotting time of human plasma contacted with virgin and PEGylated membranes was also measured as follows. Plasma was separated from other blood components by a two-step centrifugation (1st step: 1200 rpm, 10 min, 25 °C; 2nd step: 3000 rpm, 10 min, 25 °C). Plasma was then recalcified at 37 °C to 20 mM $CaCl_2$ using a 1 M stock solution. Thereafter, 0.5 mL of recalcified plasma was poured onto the membrane disks (0.4 cm^2) disposed in a 24-well plate. Absorbance at 660 nm of the solution maintained at 37 °C was continuously measured using a PowerWave microplate spectrophotometer. The plasma clotting time was determined as the time necessary to reach the onset of the absorbance transition. Experiments were repeated six times and average value for each sample taken as the plasma clotting time.

3. Results and discussion

3.1. Effect of PS_{60}-*b*-$PEGMA_{108}$ copolymer on membrane formation, physical properties and surface chemistry of PVDF membranes

3.1.1. Membrane formation aspects

The surface modification of membranes using the blending method coupled to a phase inversion process has one main disadvantage: the lack of knowledge regarding the possible effect of copolymer on membrane formation. The copolymer additive may influence (i) the composition path on a related phase diagram, and so the thermodynamic of phase separation and/or (ii) the kinetic of phase separation and polymer domains growth. As the final structure arises from the interplay of thermodynamic and kinetic phenomena, changes can be reasonably expected. Virgin PVDF membrane prepared by VIPS often present a nodular structure or a lacy structure, provided that the exposure time to water vapors is long enough to allow the formation of the nascent structure in the humidity chamber, and not in the immersion bath, which would give rise to finger-like structures. A discussion on the phenomena leading to nodules rather than to interconnected polymer domains and vice versa was presented by Wang and coworkers earlier so that according to their work, membrane formation of virgin PVDF membrane is favored by crystallization in the present study [20]. Indeed, nodules appear on the SEM picture (Fig. 1) as well as on AFM image (Fig. 2) of virgin membrane, and are still importantly present for membranes containing 1, 2 and 3 wt% copolymer additive. From 4 wt%, however, their size tends to decrease, and the structure of membrane containing 5 wt% additive is very close to be bi-continuous, structure associated to a non-crystallization gelation process. Therefore, these SEM and AFM characterizations suggest that there exists an effect of PS_{60}-*b*-$PEGMA_{108}$ on membrane structure, and that there seems to be a copolymer concentration across which the dominating membrane formation process switch from a crystallization-initiation gelling process to non-crystallization-initiation gelling.

SEM and AFM observations imply that there is a change of polymer chains conformation in the polymeric system before the initiation of phase separation. This conclusion was supported by FT-IR characterization in the lower wavenumbers region, which confirmed the change of mechanism dominating formation of PEGylated PVDF membranes containing 5 wt% PS_{60}-*b*-$PEGMA_{108}$ (Fig. 3). When membrane formation by crystallization (therefore by nodule growth) is the main phenomenon, the β-polymorph dominates (stretching band at 840 cm^{-1}) while when a non-crystallization gelling is associated to membrane formation, there is, according to Li et al.'s work, a preference for the α-form with the occurrence of a stretching band at 763 cm^{-1} [20]. Clearly a peak associated to the α-polymorph is seen on the spectrum of sample containing copolymer and its intensity tends to qualitatively increase until reaching a maximum for a 5 wt% copolymer concentration.

Even though the mechanism responsible for morphology changes when adding PS_{60}-*b*-$PEGMA_{108}$ in the PVDF casting solution is still unknown, one hypothesis can be advanced. The crystalline domain growth rate must have been hindered and even prevented, and it may be due to a change of viscosity of the casting solution. Provided that the viscosity of a polymeric solution generally increases with the polymer concentration ([21] and Supporting information), it is reasonable to assume that it rose with PS_{60}-*b*-$PEGMA_{108}$ content. An increase of the polymer concentration at the upper interface (the one between the nonsolvent atmosphere and the polymeric system) usually slows down solvent and non-solvent transfers by offering a supplementary resistant to mass transport. As a result, we suspected that it affected the polymer domain growth rate. Indeed, Tsai et al. demonstrated that an increase of a polysulfone solution viscosity delayed the domain growth and coarsening of the system leading to a retainment of pore connectivity [22]. If we apply this theory to our PVDF system, then nodule growth have been delayed by increasing copolymer content.

More evidences and investigations are needed to support this assumption and discriminate the actual phenomenon responsible for the change of membrane structure. Considering the formulation of initial solutions in the present work, the increase of viscosity due to the addition of copolymer may account for alterations of solvent and nonsolvent transfers. However, because of its amphiphilic nature, PS-*b*-PEGMA might also favor destabilization of the ternary system and so, promote water penetration. Therefore, there is undoubtedly a complex interplay between both phenomena (kinetic/thermodynamic) that points the need for further dedicated investigations.

To end, morphological and chemical studies highlighted the formation of bi-continuous structure at high copolymer content, structure which is highly desired for UF and MF applications of membranes. Indeed, it offers high connectivity between polymer-lean domains, which means that high permeability can be expected, as well as high connectivity of the polymer-rich phase, offering good mechanical properties to the membrane.

3.1.2. Physical properties of membranes

Consequences of the change of structure on physical properties of membranes are numerous. In particular, mechanical properties can be affected. Herein, both the change of morphology, and the increase of total polymer content led to an improvement of stiffness and ductility of PVDF membranes, but it is unclear however which effect dominated the improvement observed. Fig. 4 and Table 2 reveal that the modulus of elasticity, along with the tensile strength of membranes and the elongation at break tended to increase with the copolymer content, unveiling stiffer and more ductile membranes. To the best of our knowledge, only two studies mentioned the testing of similar mechanical properties of PVDF membranes prepared by VIPS [20,23]. In particular, tensile strength was reported by Peng et al. to decrease with exposure time to non-solvent vapors, and felt below 1 MPa after 10 min. Herein, exposure time to water vapors was 20 min, and tensile strength of virgin membrane was about 1 MPa, which is consistent with Peng et al.'s study, considering that we used a larger polymer concentration in the casting solution (20 wt% vs. 15 wt%), therefore leading to better mechanical properties [23]. Values of tensile strength is also in accordance with those obtained by Li et al. for PVDF membranes prepared by VIPS in similar conditions of polymer dissolution temperature, relative humidity and exposure time to non-solvent vapors [20]. Note however that we

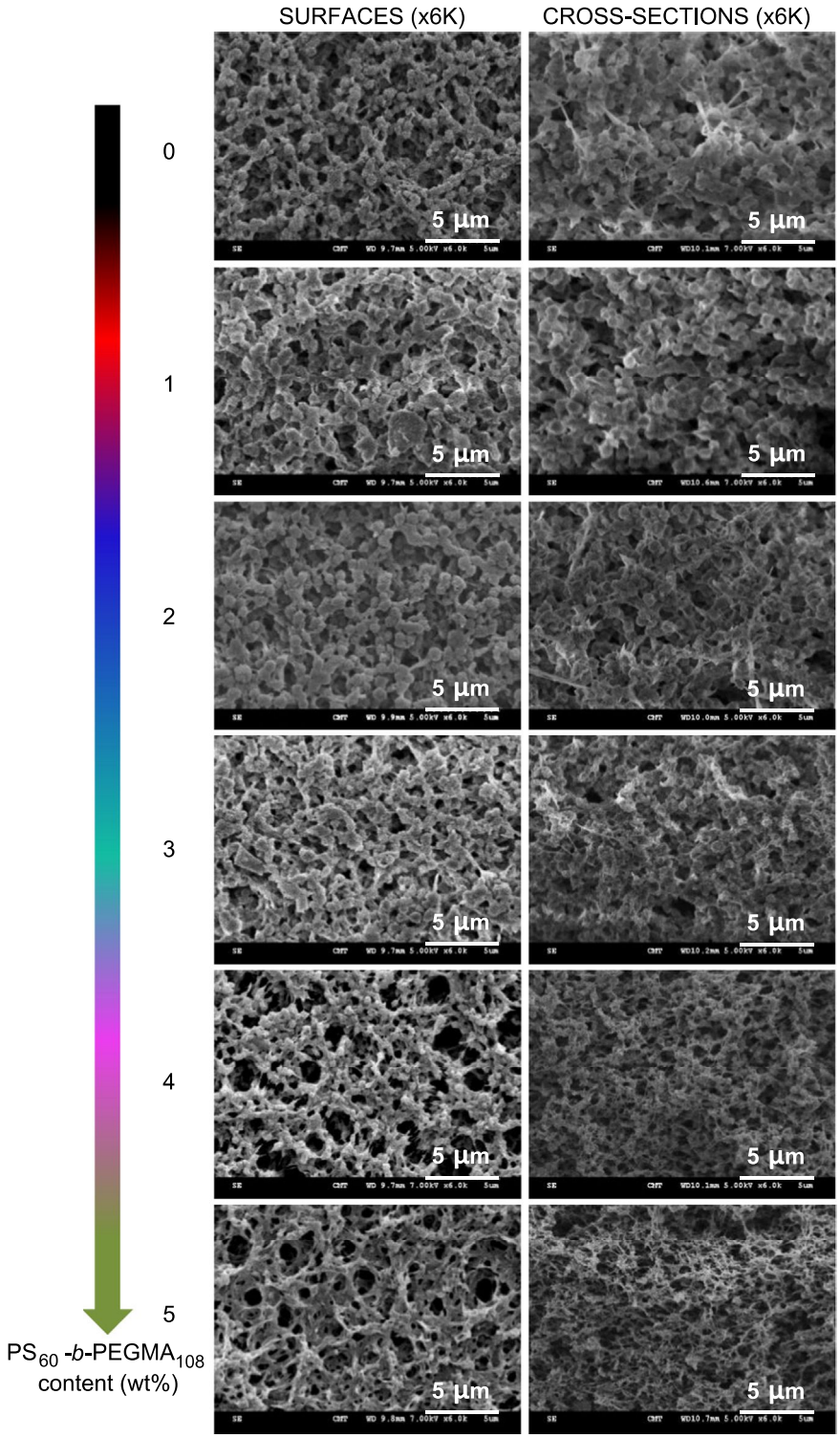

Fig. 1. SEM characterization of virgin PVDF and PEGylated PVDF membranes.

measured lower modulus of elasticity for virgin PVDF membrane (22.3 ± 5.4 MPa vs. 56 ± 12 MPa). Indeed, in similar operating conditions but using a different material (and so a different PVDF molecular weight), Li et al. obtained bi-continuous virgin PVDF membranes which probably accounts for this difference [20]. Moreover, modified membranes clearly displayed higher tensile strengths. Finally, more ductile matrices were obtained increasing the copolymer content as elongation at break for Mod-5 membrane was greater than that of the virgin PVDF membrane.

In sum, our result confirm that well-connected polymer domains as in bi-continuous structures offer better mechanical properties than structures loosely connected such as nodular membranes. Further, higher dry-matter content (Mod-5 membrane) in the original polymer/copolymer/solvent system obviously leads to membranes with more important polymer-rich domain, compares with virgin PVDF membrane, and so to better modulus of elasticity and tensile strength.

Finally, pore size and porosity measurements revealed that membranes' pore size tended to decrease with copolymer additive but still

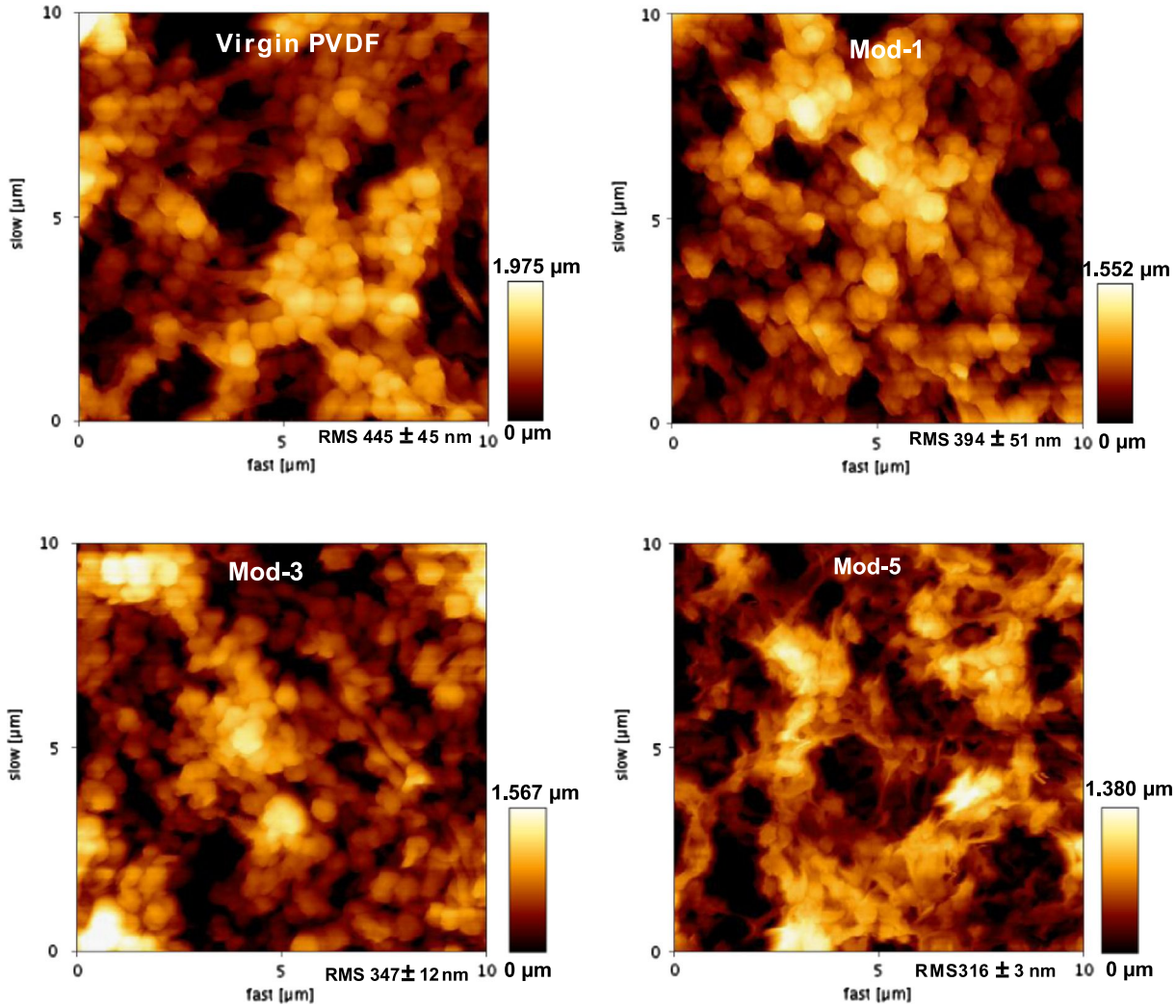

Fig. 2. 10 µm × 10 µm AFM characterization of virgin PVDF and PEGylated PVDF membranes. *RMS coefficients were obtained from 3 to 5 analyses, including that presented here.*

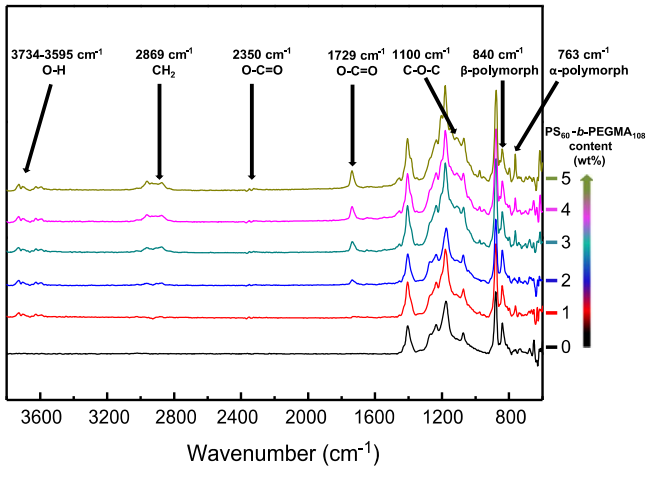

Fig. 3. FT-IR chemical analysis of virgin PVDF and PEGylated PVDF membranes.

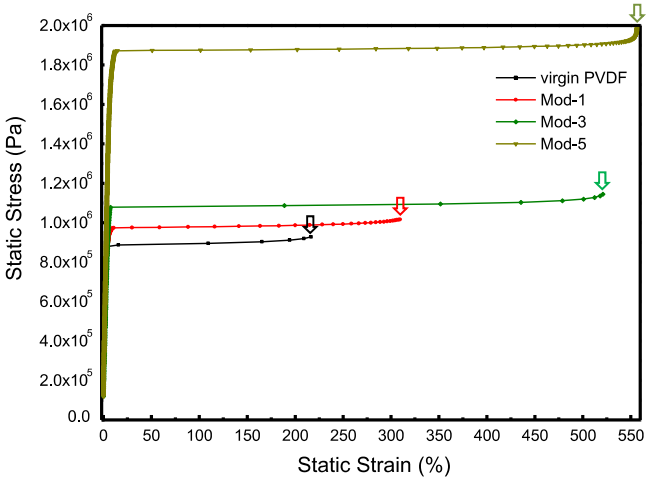

Fig. 4. Stress–strain plots of virgin PVDF and Mod-5 membranes. *The arrows highlight membrane failure.*

remained in the lower region of MF domain, while the porosity of membranes remained high and in the same range (67–71%) (Table 2). The slight decreasing of pore size was probably due to the increase of total polymer (PVDF and PS_{60}-*b*-$PEGMA_{108}$) content, while the steady porosity unveiled an expansion of the polymer-lean phase, which would be consistent with an improvement of water diffusion during membrane formation, as above discussed.

3.1.3. *Analysis of the surface chemistry of membranes*

To complete this study on physico-chemical characterization of membranes, further details can be provided regarding the surface chemistry of membranes. Results of both FT-IR (Fig. 3) and XPS (Fig. 5) analyses confirm that PS_{60}-*b*-$PEGMA_{108}$ is present at the

surface of membranes. Besides the change of prevailing crystalline polymorph evidenced in the fingerprint region, FT-IR analysis revealed the presence of an absorption band at 1100 cm^{-1}, attributed to the stretching of C–O–C group. In addition, the absorption band at 1729 cm^{-1} and the slight signal at 2350 cm^{-1} were attributed to the stretching of carbonyl functions held by PEGMA segments, and confirm the presence of PS_{60}-*b*-$PEGMA_{108}$ at the surface of the membranes [24,25]. The presence of an absorption band at 2869 cm^{-1} was also noted, due to the stretching vibration of CH_2 groups carried by PEGMA hydrophilic heads, along with a broad signal in the range 3595–3734 cm^{-1} attributed to OH vibration. Further, XPS analysis did evidence an overall increase of oxygen content onto the surfaces of membranes (Fig. 5). This result is due to both an increase of copolymer content but also to the migration of copolymer to the surface of membranes during membrane formation in order to reduce the surface energy. Though it is not clear in which extent migration occurs, it is reasonable to state that it will be favored at higher PS_{60}-*b*-$PEGMA_{108}$, especially if VIPS is used rather than LIPS which fixes more quickly the structure, leading to a dense surface coverage. In this respect a better surface coverage by PS_{60}-*b*-$PEGMA_{108}$ is obtained by VIPS. One should note however that the migration also depends on the extent of interactions between PS groups and PVDF chains. Reducing the number of styrene units would probably further optimize the motion of copolymer, but also weaken their entanglement with PVDF chains, which is obviously not desired for a stability concern.

Table 2
Physical properties of membranes.

Membrane ID	Modulus of elasticity (MPa)	Tensile strength at break (MPa)	Mean pore flow diameter (μm)	Porosity (%)
Virgin PVDF	22.3 ± 5.4	0.97 ± 0.04	0.197 ± 0.003	70.9 ± 2.4
Mod-1	21.9 ± 4.1	0.98 ± 0.05	0.179 ± 0.006	67.4 ± 2.1
Mod-3	23.6 ± 0.7	1.25 ± 0.15	0.161 ± 0.001	71.0 ± 3.4
Mod-5	31.6 ± 8.4	1.85 ± 0.04	0.102 ± 0.001	67.1 ± 2.0

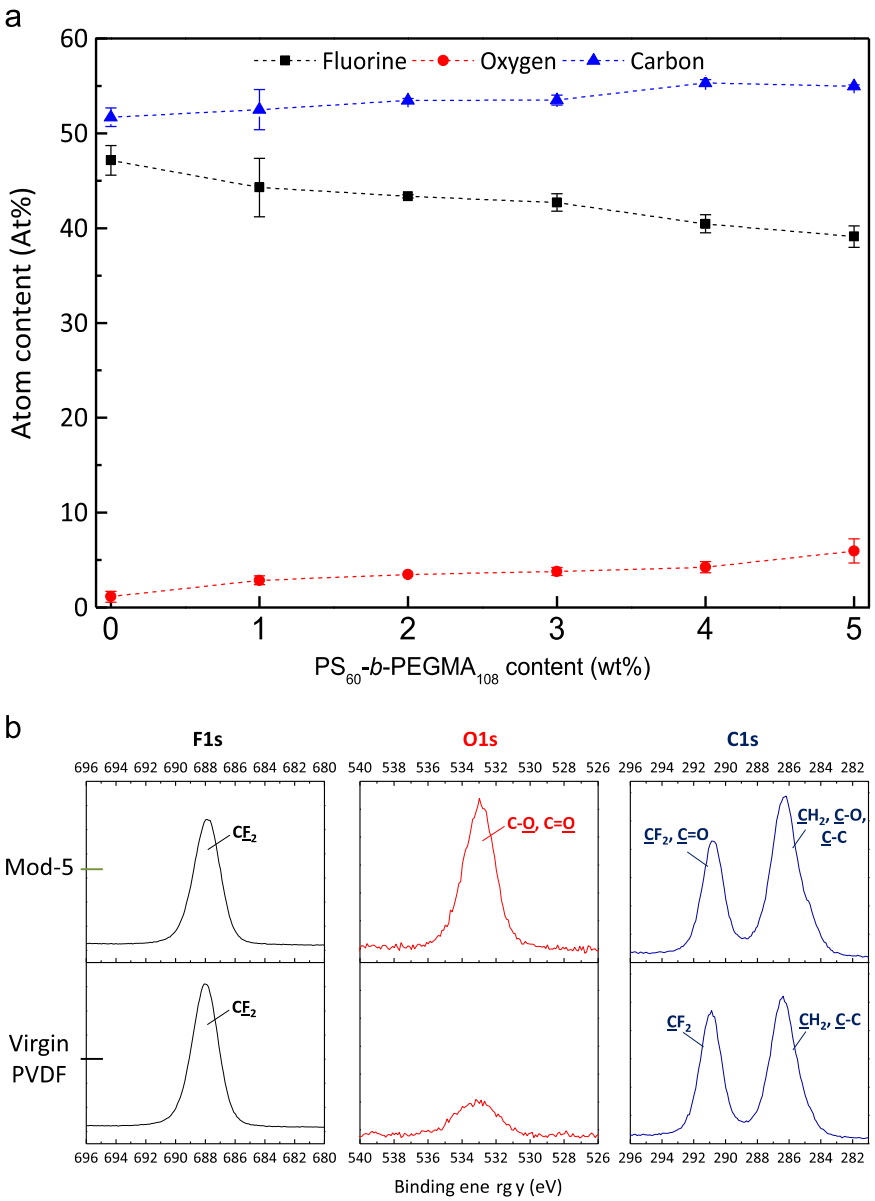

Fig. 5. XPS analysis of virgin PVDF and PEGylated PVDF membranes. (a) Element composition as a function of copolymer content; (b) core-level spectra of virgin PVDF and Mod-5 membranes.

3.2. *Effect of PS_{60}-b-$PEGMA_{108}$ copolymer on biofouling of PVDF membranes at nano- and micro-scales*

Hemocompatible membranes must efficiently resist biofouling due to proteins and bacteria because both can mediate undesired biological responses and infections when membrane is contacted with blood [26,27]. A major difficulty arising when designing an antibiofouling or at least a low-biofouling membrane is linked to the different "fouling scales" – nano- for proteins and micro- for bacteria – involved. In general, the literature proves that a surface resisting the adhesion of proteins will also prevent bacterial attachment [28,29]. The converse however is false, due to characteristic sizes involved. One should also note that most studies on the design of antifouling surfaces or membranes are carried out on rather smooth surfaces, so that there is minor physical effect on fouling. Herein, membranes are very rough and so, favorable to the physical entrapment of biofoulants. A prerequisite to resist fouling however, whatever the physical state of the surface, is its ability to entrap water and form a protective hydrophilic layer [5,30].

3.2.1. *Hydration properties of membranes*

In this study, membranes' surface water contact angle was not drastically reduced as seen in Fig. 6, but hydration capacity was importantly increased with the copolymer content, resulting from numerous interactions between water molecules and hydrophilic segments. To analyze the hydrophilicity of a surface, here through the value of the water contact angle, one has to consider the complex interplay between both the surface physical state (roughness, porosity) and the surface chemistry. The trend obtained for water contact angle can be mostly attributed to the membrane preparation process and morphologies obtained. A positive correlation between the extent of crystallinity and hydrophobicity is suspected, even though we lack of evidences to support this assumption. Therefore, by favoring nodule growth, hydrophobicity of membranes may increase as well, through the formation of a secondary indented structure onto nodules promoting the entrapment of air. In addition, lacy structures are also very rough and very porous, as highlighted by the RMS coefficient on AFM images (Fig. 2), therefore enabling air trapping. As virgin PVDF membrane displayed a typical nodular structure, very rough and porous, a quite high water contact angle was obtained. The addition of PS_{60}-*b*-$PEGMA_{108}$ did not significantly affect the structure of membranes at low copolymer content. Therefore, water contact angles were still high. For high copolymer contents (4–5 wt%), a concomitant effect of addition of PS_{60}-*b*-$PEGMA_{108}$ on surface chemistry and surface morphology arose in a slight reduction of water contact angle of about 10°, compared with that of virgin PVDF membrane. After a 24-h immersion period in DI water however, the chemical effect became predominant over the physical one, resulting in an overall important increase of membranes hydration. This property is essential for membranes to resist biofouling, rather than surface water contact angle, important for the design of antifouling dense coatings for instance. Indeed, not only the surface but the whole matrix is challenged in the case of MF/UF membranes.

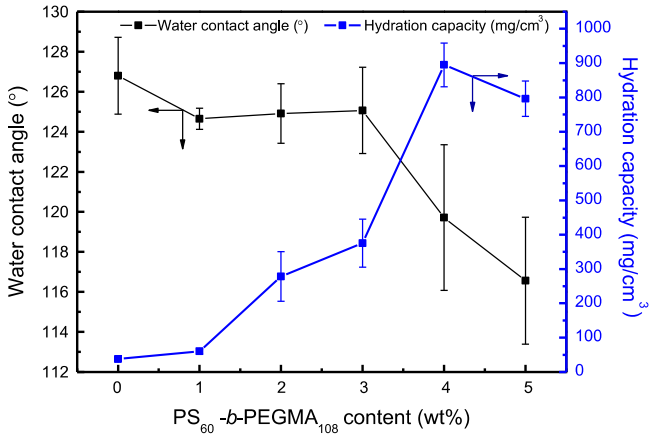

Fig. 6. Hydrophilic properties of virgin PVDF membrane and PEGylated PVDF membranes. Note that hydration capacity is expressed per unit of porous volume. The later was evaluated after measuring the thickness of each sample (virgin: 98 ± 11 μm; Mod-1: 93 ± 16 μm; Mod-2: 92 ± 8 μm; Mod-3: 98 ± 17 μm; Mod-4: 95 ± 2 μm; Mod-5: 81 ± 4 μm) and from the knowledge of their total initial surface area and porosity.

3.2.2. *Effect of PS_{60}-b-$PEGMA_{108}$ copolymer on resistance of membranes to protein adsorption*

Then, the resistance to biofouling at a nano-scale was investigated, using three model proteins, BSA, LY and FN. Results of these tests are presented in Fig. 7 and in associated content (Fig. S1). Two points should be highlighted at first. There is clearly an important reduction of protein adsorption (LY: 93%; BSA: 89%; FN 73%) with copolymer content and whatever the modified membrane, it resists more efficiently LY adsorption than BSA adsorption, while it is less efficient to inhibit FN adsorption. The first statement in particular is important regarding our initial objective. Antifouling resistance is ascribed to strong repulsive forces arising from the formation of a hydrated layer surrounding PS_{60}-*b*-$PEGMA_{108}$ and it is worth noticing the important correlation between hydrophilic capacity and protein adsorption by comparing Figs. 6 and 7. The second statement unveils the difficulty to design a "universal" antibiofouling matrix. A number of parameters can drastically influence protein adsorption among which (i) the nature of the protein, (ii) the chemical state of the surface and (iii) the physical state of the surface. The overall deceasing of protein adsorption is attributed to a change of both the chemical and physical states of the membranes surface. However, we suspect that the nature of the protein was the major parameter explaining why PEGylated membranes were more efficient to resist LY. LY is a rather small protein so that its diffusion toward potential adsorption sites is facilitated. However, it is probably less hydrophobic than BSA and FN proteins which have higher molecular weights. So, it might be less likely to interact with PVDF. In opposition, FN is a sticky large molecular weight protein, and therefore diffuses more slowly than LY and BSA. Nevertheless, it contains much more potential anchoring sites, so that it can easily interact with membranes. Resistance to its adsorption was found

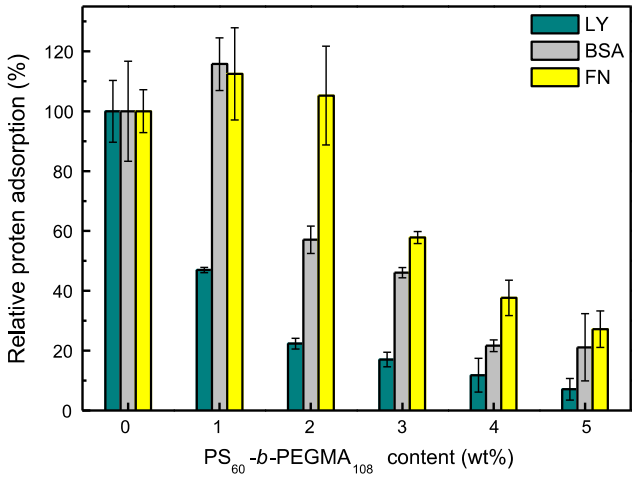

Fig. 7. Relative adsorption of fibrinogen, bovine serum albumin and lysozyme onto virgin PVDF membrane and PEGylated PVDF membranes.

to be around 73%, which is one of the best results reported for such a rough matrix. It would be interesting to investigate the exact location of proteins adsorption: at the surface or in the deeper layers, to support this discussion on the effect of protein molecular weight on protein adsorption. Also, from the results of XPS analysis presented earlier in Fig. 5 and in Table S2, optimal resistance to nano-fouling corresponds to a minimum oxygen atom content at the surface of about 4.2%. Finally, one should note that despite the obtaining of rough membranes whatever the copolymer content, a slight decrease of RMS coefficient occurred when switching from virgin PVDF to Mod-5 membranes (Fig. 2), which is also favorable to an improvement of resistance to nano-biofouling, even though this was clearly not the dominant effect.

3.2.3. *Effect of PS_{60}-b-$PEGMA_{108}$ copolymer on resistance of membranes to bacterial attachment*

As tests regarding resistance to biofouling at a nano-scale provided positive results, attachment of bacteria was assessed and results displayed in Fig. 8 and in the associated content (Figs. S2 and S3). Whether using *S. epidermidis* or *E. coli*, bacterial adhesion was almost totally inhibited for membranes containing 4 and 5 wt% copolymer content. We have stressed earlier that resistance to biofouling at a nano-scale often leads to biofouling resistance at a macro-scale. However, these tests had to be undertaken because of the possibility of bacterial entrapment within the nodules. Some bacteria, in particular gram-negative ones, have a rather thin outer cell wall. Therefore, they are flexible and can modify their shape to interact with a surface and penetrate within pores. These qualitative results highlight the good quality of chemical modification in terms of copolymer content, homogeneous dispersion and surface coverage.

3.3. *Hemocompatibility of membranes*

A material is hemocompatible if after contact with blood, no blood cell disruption nor biological responses are inferred. In particular, the material should not interact with erythrocytes, leukocytes or thrombocytes. It is generally accepted that plasma proteins, and in particular fibrinogen, mediate interactions with blood cells and lead to blood clotting [24,31,32]. In the previous section, we found that fibrinogen adsorption was drastically reduced. It was not reduced to 100% the limitation of the virgin membrane, but Mod-5 membrane exhibited a resistance to FN adsorption only slightly inferior to that of a sulfobetaine methacrylate hydrogel, a very hydrophilic surface (Fig. S1). As FN is one among dozens of proteins in plasma, and so less likely to interact with membranes like pure FN in ELISA tests does, it was thought that PEGylated membranes could present improved hemocompatibility, compared to virgin matrix. This potential hemocompatibility was supported by resistances measured to the adhesion of other plasma proteins, including γ-globulin and human-serum-albumin, as well as by the resistance to the adsorption of fibrinogen contained in a platelets-poor-plasma solution (Fig. S1).

3.3.1. *Evaluation of the resistance of membranes to blood cells adhesion*

Blood cells adhesion was tested and results are presented in Fig. 9. Notice that results shown are 3D confocal images, while the related 2D images are also provided in Supporting information section, revealing the detection of the membrane porous structure (corresponding to reddish shapes onto 3D pictures). The extent of cell–membrane interactions depends partly on the nature of the cell tested, as shown by images related to virgin PVDF membrane. It appears that virgin PVDF presents partial hemocompatibility since despite numerous interactions with leukocytes, not many erythrocytes or thrombocytes were found onto the surface or within the deeper layers of the porous matrix. This behavior may be ascribed to the different natures of the biological cell membrane arising in dissimilar adsorption behaviors onto synthetic polymer. It is also important noting that up to a 3 wt% copolymer concentration, no general decreasing of blood cells adhesion could be observed. Only membranes containing 5 wt% copolymer presented an important resistance to all types of cells. Therefore, Mod-5 membranes do present improved hemocompatibility property. In particular, there are almost no erythrocytes or thrombocytes on the surface and within the membrane, observation that can be correlated to results of Fig. 8. As aforementioned and reminded by Corum et al., fibrinogen is considered as the main protein responsible for platelet activation leading to the formation of a thrombus once blood has been contacted with a surface [31]. So, by designing a PVDF membrane efficiently resisting FN adsorption thanks to a dense and homogeneous copolymer distribution, the probability of thrombocytes to be activated is reduced.

Furthermore, alike for the resistance to bacteria attachment, the adhesion of cells can be mediated by the physical nature of the surface and that of the matrix. A rough surface facilitates the entrapment of cells, and it is therefore recommended to optimize the copolymer surface density, to balance the undesirable physical effect. In addition, our results show that blood cells can be entrapped inside pore which diameter is smaller than the characteristic length of the cells. Herein, a physical trapping inside the membrane was a priori not expected, considering the size of the cells (ranging between 1 and 17 μm depending on the nature of the blood cell) and the pores dimensions (Table 2). Interestingly, 3D confocal image highlighted that numerous cells were actually entrapped inside the membrane. In particular, leukocytes, the largest blood cells, easily penetrated into the matrix, highlighting

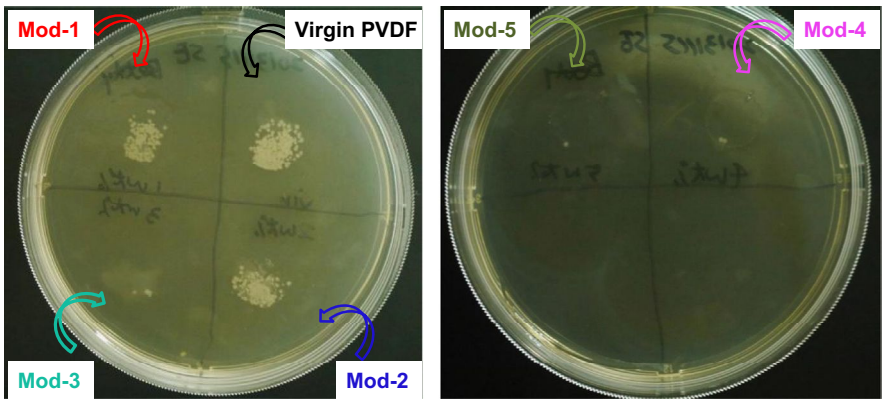

Fig. 8. Resistance of PEGylated membranes to the adhesion of *Staphylococcus epidermidis*.

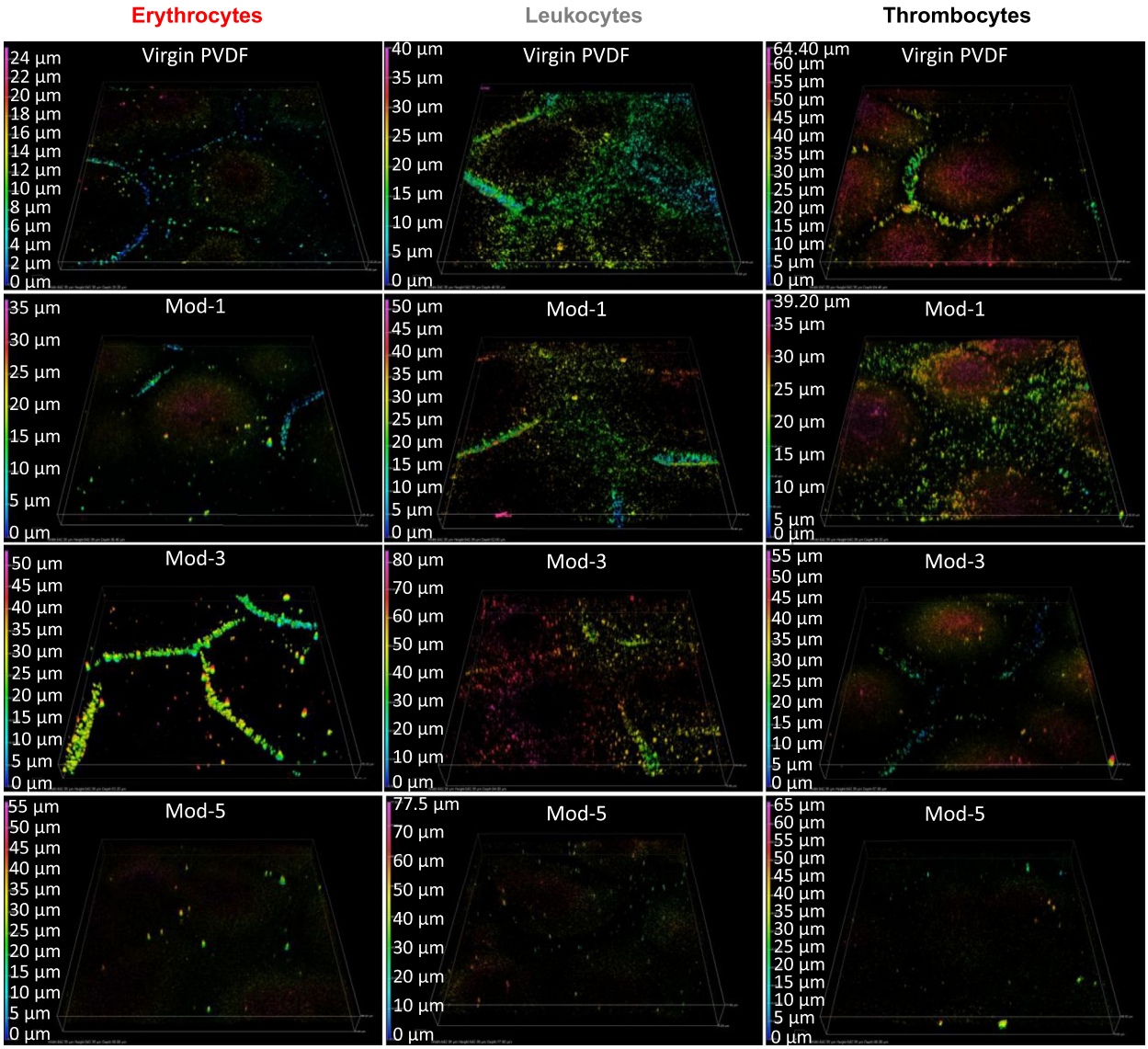

Fig. 9. Blood cells adhesion tests onto virgin PVDF and PEGylated PVDF membranes. *x*-Scale (width) and *y*-scale (height) for each image was 642.39 μm; *z*-scale varied depending on the depth of the last cells detected during analysis of a given sample.

their cell-wall deformability and so, the need for an important antibiofouling agent concentration within the membrane. Mod-5 membranes meet this requirement but also have the lowest mean pore flow size, which has probably played a role in preventing cell penetration, and their subsequent organization inside the furrows formed by the porous structures, as observed for instance in Mod-3 membrane (image related to RBCs adhesion). We therefore conclude from these images and correlations with data above mentioned that a 5 wt% PS_{60}-*b*-$PEGMA_{108}$ concentration is absolutely required to prevent blood cell attachment, whatever their nature, along with smaller pore size, in order to intend balancing the physical penalty offered to trapping. Notice also that this measurement of hemocompatibility corresponds to an oxygen atom content of about 6% (Fig. 5, Table S2).

3.3.2. *Extent of hemolytic activity and thrombosis after blood contact with membranes*

Another important test to assess hemocompatibility of a surface is the hemolysis ratio. Hemolysis refers to the amount of red blood cells which membrane will be ruptured leading to the release of the cytoplasm including hemoglobin. Hemolysis can be caused by a number of conditions, including the presence of bacteria, which also supports the need for designing membranes resisting bacterial attachment. Herein, the extent of hemolysis following blood contact with membranes was assessed and compared with hemolysis ratio obtained after contacting blood with PBS (no lysis) and DI water (100% lysis). Related results are presented in Fig. 10. In general, a material is considered as potentially hemocompatible if the hemolysis ratio is lower than 5% [33,34]. Our results indicate that PVDF membrane does not mediate the lysis of red blood cells in an important extent and therefore suggest that the PVDF membrane prepared by VIPS is biocompatible and could be potentially used as a material for blood filtration devices for instance. However, improvement is required as above discussed, and PS_{60}-*b*-$PEGMA_{108}$ allowed enhancing the membranes biocompatibility as hemolysis ratio was reduced from about 2.25% for the virgin PVDF matrix to less than 1.0% for PEGylated membranes prepared from casting solution containing more than 1 wt% copolymer. Notice that considering the average values obtained and the error limits associated to these data, a plateau was reached from Mod-2 membrane, indicating that a 2 wt% copolymer concentration in the initial casting solution is enough to prevent cell lysis. Despite an

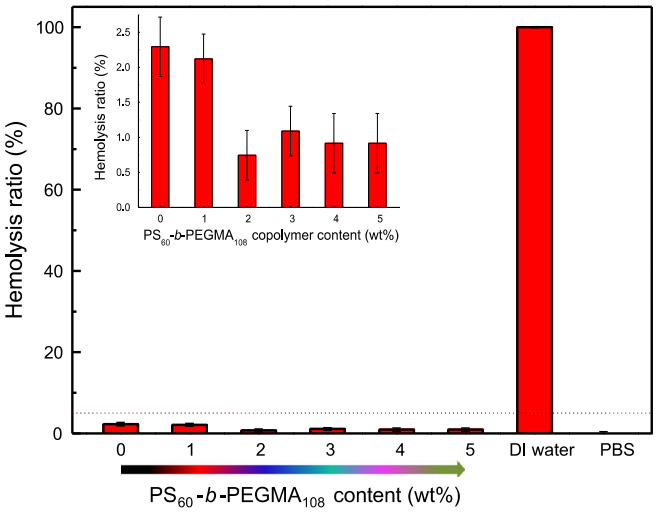

Fig. 10. Hemolysis of RBCs in the presence of virgin PVDF and PEGylated PVDF membranes. *The inset better highlights the effect of copolymer on hemolysis ratio.*

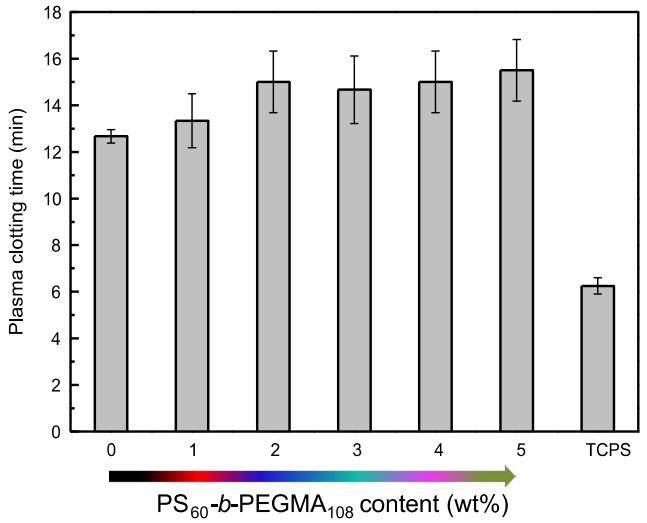

Fig. 11. Plasma clotting time of recalcified platelet-poor plasma in the presence of virgin PVDF and PEGylated PVDF membranes.

apparent lack of knowledge and lack of literature available on the hemocompatibility of PVDF membranes, we can compare the present data with previously published work by Chang and coworkers [35]. In particular, they investigated the hemocompatibility of PVDF membranes grafted with sulfobetaine and reported a hemolysis ratio of about 18% with virgin commercial PVDF membrane. This is about 8 times the value found in this study. It should be noted however that the nature of the membrane used by Chang and coworkers was different from that used in the present work. In particular, their commercial membrane exhibited a lacy structure.

Finally, plasma clotting time was tested to assess the anticoagulant activity of PS_{60}-*b*-$PEGMA_{108}$. Results displayed in Fig. 11 are in accordance with other hemocompatibility tests, that is, the copolymer delays the clotting time, therefore revealing its positive effect on hemocompatibility. Again, very few work reported on the clotting time of plasma contacted with microporous PVDF membranes. As for hemolysis, we found that our virgin PVDF presented a clotting time (12.5 ± 0.5 min) higher than those reported earlier for commercial PVDF membrane (10 ± 0.5 min [35] and 2.5 ± 1.5 min [18]), which suggests a certain degree of hemocompatibility of virgin PVDF membranes. The chemical nature of PVDF (Mw) as well as the membrane structure may account for these differences. We also observed in our study a delay of clotting time longer using PS_{60}-*b*-$PEGMA_{108}$ as a surface-modifier rather than grafted PSBMA, yet known as an outstanding antibiofouling and potentially hemocompatible polymer (15.5 ± 1 min vs. 14 ± 2 min) [35]. The improvement however, is not as good as that reported earlier, because our virgin PVDF membranes do present some characteristics of hemocompatible surfaces. In addition, clotting tine was in the same range as that obtained after a 15-s atmospheric plasma treatment of a PVDF commercial membrane coated with PEGMA monomer, and leading to PVDF-*g*-PEGMA membranes (15 ± 1 min) [18]. This result along with other tests on blood compatibility suggest that the modification in situ of PVDF membranes by PS_{60}-*b*-$PEGMA_{108}$ and the use of VIPS as a membrane preparation process provide an efficient, competitive, cost-effective and readily achieved one-step alternative to surface modification processes, for the preparation of hemocompatible membranes.

4. Conclusion

In the present paper, we presented a one-step formation and in situ modification by PS_{60}-*b*-$PEGMA_{108}$ copolymer of PVDF membranes using VIPS process. These novel membranes are intended to be used for their improved hemocompatibility. Main conclusions are as follows:

- An important effect of PS_{60}-*b*-$PEGMA_{108}$ on membrane formation mechanisms was observed. In particular, an increase of PS_{60}-*b*-$PEGMA_{108}$ content was accompanied by a modification of the porous structure from nodular to bi-continuous, which was supported by a change of main crystalline polymorph present at the membrane surface (β-polymorph for virgin PVDF membrane, α-polymorph for PEGylated PVDF membrane prepared from a solution containing 5 wt% copolymer).
- The copolymer importantly improved overall hydration of membranes, despite a rather small decreasing of water contact angle attributed to a negative physical effect. Therefore, PS_{60}-*b*-$PEGMA_{108}$ copolymer significantly enhanced the resistance of membranes to biofouling at a nano-scale (using bovine-serum-albumin, lysozyme and fibrinogen proteins) and a macro-scale (tests performed with *S. epidermidis* and *E. coli*).
- Hemocompatibility assessed using a number of cell adhesion tests including erythrocytes, leukocytes and thrombocytes adhesion, as well as by evaluating hemolysis ratio after contact with membranes and plasma clotting time, revealed that membranes containing 5 wt% copolymer are highly hemocompatible (no cell adhesion, 1% hemolysis ratio and 16-min plasma clotting time), suggesting their possible use in blood filtration.

Acknowledgments

The authors wish to express their sincere gratitude to the National Science Council Taiwan (NSC 103-2221-E-033-074) and to the 2013–2015 NSC-ANR Blanc International II Program (Taiwan–France Project: Super-NAM, ANR-12-IS08-0002 and NSC 102-2923-E-033-001-MY3) for their financial support.

Appendix A. Supporting information

Supplementary data associated with this article can be found in the online version at http://dx.doi.org/10.1016/j.memsci.2014.07.014.

References

[1] D.F. Stamatialis, B.J. Papenburg, M. Gironés, S. Saiful, S.N.M. Bettahalli, S. Schmitmeier, M. Wessling, Medical applications of membranes: drug delivery, artificial organs and tissue engineering, J. Membr. Sci. 308 (2008) 1–34.

[2] M.A. Wassall, M. Santin, G. Peluso, S.P. Denver, Possible role of α-1-microglobulin in mediating bacterial attachment to model surfaces, J. Biomed. Mater. Res. 40 (1998) 365–370.

[3] A.R. Statz, A.E. Barron, P.B. Messersmith, Protein, cell and bacterial fouling resistance of polypeptoid-modified surfaces: effect of side-chain chemistry, Soft Matter 4 (2008) 131–139.

[4] M. Mulder, Materials and material properties, Basic Principles of Membrane Technology, 2nd ed., Kluwer Academic Publishers, Dordrecht, The Netherlands (1997) 51–59.

[5] D. Rana, T. Matsuura, Surface modifications for antifouling membranes, Chem. Rev. 110 (2010) 2448–2471.

[6] H.J. Yu, Y.M. Cao, G.D. Kang, M.Q. Zhou, J.H. Liu, Q. Yuan, Enhancing antifouling property of polysulfone ultrafiltration membrane by grafting poly(ethylene glycol) methyl ether methacrylate(PEGMA) via UV-initiated polymerization, Chem. J. Chin. Univ. 31 (2010) 2506–2510.

[7] S. Zanini, M. Müller, C. Riccardi, M. Orlandi, Polyethylene glycol grafting on polypropylene membranes for anti-fouling properties, Plasma Chem. Plasma Process. 27 (2007) 446–457.

[8] D.G. Kim, H. Kang, S. Han, J.C. Lee, The increase of antifouling properties of ultrafiltration membrane coated by star-shaped polymers, J. Mater. Chem. 22 (2012) 8654–8661.

[9] Y.Q. Wang, Y.L. Su, Q. Sun, X.L. Ma, Z.J. Jiang, Generation of anti-biofouling ultrafiltration membrane surface by blending novel branched amphiphilic polymers with polyethersulfone, J. Membr. Sci. 286 (2006) 228–236.

[10] T. Wang, Y.Q. Wang, Y.L. Su, Z.Y. Jiang, Antifouling ultrafiltration membrane composed of polyethersulfone and sulfobetaine copolymer, J. Membr. Sci. 280 (2006) 343–350.

[11] A. Venault, Y.H. Liu, J.R. Wu, H.S. Yang, Y. Chang, J.Y. Lai, P. Aimar, Low-biofouling membranes prepared by liquid-induced phase separation of the PVDF/polystyrene-b-poly (ethylene glycol) methacrylate blend, J. Membr. Sci. 450 (2014) 340–350.

[12] G.R. Guillen, Y. Pan, M. Li, E.M.V. Hoek, Preparation and characterization of membranes formed by nonsolvent induced phase separation: a review, Ind. Eng. Chem. Res. 50 (2011) 3798–3817.

[13] Y.C. Chiag, Y. Chang, W.Y. Chen, R.C. Ruaan, Biofouling resistance of ultrafiltration membranes controlled by surface self-assembled coating with PEGylated copolymers, Langmuir 28 (2012) 1399–1407.

[14] N.J. Lin, H.S. Yang, Y. Chang, K.L. Tung, W.H. Chen, H.W. Cheng, S.W. Hsiao, P. Aimar, K. Yamamoto, J.Y. Lai, Surface self-assembled PEGylation of fluoro-based PVDF membranes via hydrophobic-driven copolymer anchoring for ultra-stable biofouling resistance, Langmuir 29 (2013) 10183–10193.

[15] S.T. Kao, M.Y. Teng, C.L. Li, C.Y. Kuo, C.Y. Hsieh, H.A. Tsai, D.M. Wang, K.R. Lee, J. Y. Lai, Fabricating PC/PAN composite membranes by vapor-induced phase separation, Desalination 233 (2008) 96–103.

[16] M. Gu, J. Zhang, X. Wang, H. Tao, L. Ge, Formation of poly(vinylidene fluoride) (PVDF) membranes via thermally induced phase separation, Desalination 192 (2006) 160–167.

[17] J. Zhang, Z. Song, B. Li, Q. Wang, S. Wang, Fabrication and characterization of superhydrophobic poly(vinylidene fluoride) membrane for direct contact membrane distillation, Desalination 324 (2013) 1–9.

[18] Y. Chang, Y.J. Shih, C.Y. Ko, J.F. Jhong, Y.L. Liu, T.C. Wei, Hemocompatibility of poly(vinylidene fluoride) membrane grafted with network-like and brush-like antifouling layer controlled via plasma-induced surface PEGylation, Langmuir 27 (2011) 5445–5455.

[19] C. Zhao, X. Li, L. Li, G. Cheng, X. Gong, J. Zheng, Dual functionality of antimicrobial and antifouling of poly(N-hydroxyethylacrylamide)/salicylate hydrogels, Langmuir 29 (2013) 1517–1524.

[20] C.L. Li, D.M. Wang, A. Deratani, D. Quemener, D. Bouyer, J.Y. Lai, Insight into the preparation of poly(vinylidene fluoride) membranes by vapor-induced phase separation, J. Membr. Sci. 361 (2010) 154–166.

[21] D.W. Chae, M.H. Kim, B.C. Kim, Temperature dependence of the rheological properties of poly(vinylidene fluoride)/dimethyl acetamide solutions and their electrospinning, Korea Aust. Rheol. J. 22 (2010) 229–234.

[22] J.T. Tsai, Y.S. Su, D.M. Wang, J.L. Kuo, J.Y. Lai, A. Deratani, Retainment of pore connectivity in membranes prepared with vapor-induced phase separation, J. Membr. Sci. 362 (2010) 360–373.

[23] Y. Peng, H. Fan, Y. Dong, Y. Song, H. Han, Effects of exposure time on variations in the structure and hydrophobicity of polyvinylidene fluoride membranes prepared via vapor-induced phase separation, Appl. Surf. Sci. 258 (2012) 7872–7881.

[24] J. Jin, W. Jiang, Q. Shi, J. Zhao, J. Yin, P. Stagnaro, Fabrication of PP-g-PEGMA-g-heparin and its hemocompatibility: from protein adsorption to anticoagulant tendency, Appl. Surf. Sci. 258 (2012) 5841–5849.

[25] L.P. Zhu, Y.Y. Xu, H.B. Dong, Z. Yi, B.K. Zhu, Amphiphilic PPESK-graft-P(PEGMA) copolymer for surface modification of PPESK membranes, Mater. Chem. Phys. 115 (2009) 223–228.

[26] W.B. Tsai, J.M. Grunkemeier, T.A. Horbett, Human plasma fibrinogen adsorption and platelet adhesion to polystyrene, J. Biomed. Mater. Res. 44 (1999) 130–139.

[27] K.H.A. Lau, C. Ren, T.S. Sileika, S.H. Park, I. Szleifer, P.B. Messersmith, Surface-grafted polysarcosine as a peptoid antifouling polymer brush, Langmuir 28 (2012) 16099–16107.

[28] J. Kuang, P.B. Messersmith, Universal surface-initiated polymerization of antifouling zwitterionic brushes using a mussel-mimetic peptide initiator, Langmuir 28 (2012) 7258–7266.

[29] C. Zhao, J. Zheng, Synthesis and characterization of poly(N-hydroxyethylacrylamide) for long-term antifouling ability, Biomacromolecules 12 (2011) 4071–4079.

[30] J. Peng, Y. Su, W. Chen, X. Zhao, Z. Jiang, Y. Dong, Y. Zhang, J. Liu, X. Fan, Antifouling membranes prepared by a solvent-free approach via bulk polymerization of 2-hydroxyethyl methacrylate, Ind. Eng. Chem. Res. 52 (2013) 13137–13145.

[31] L.E. Corum, C.D. Eichinger, T.W. Hsiao, V. Hlady, Using microcontact printing of fibrinogen to control surface-induced platelet adhesion and activation, Langmuir 27 (2011) 8316–8322.

[32] W.H. Kuo, M.J. Wang, H.W. Chien, T.C. Wei, C. Lee, W.B. Tsai, Surface modification with poly(sulfobetaine methacrylate-co-acrylic acid) to reduce fibrinogen adsorption, platelet adhesion, and plasma coagulation, Biomacromolecules 12 (2011) 4348–4356.

[33] L.P. Amarnath, A. Srinivas, A. Ramamurthi, In vitro hemocompatibility testing of UV-modified hyaluronan hydrogels, Biomaterials 27 (2006) 1416–1424.

[34] M. Li, K.G. Neoh, L.Q. Xu, R. Wang, E.T. Kang, T. Lau, D.P. Olszyna, E. Chiong, Surface modification of silicone for biomedical applications requiring long-term antibacterial, antifouling, and hemocompatible properties, Langmuir 28 (2012) 16408–16422.

[35] Y. Chang, W.J. Chang, Y.J. Shih, T.C. Wei, G.H. Hsiue, Zwitterionic sulfobetaine-grafted poly(vinylidene fluoride) membrane with highly effective blood compatibility via atmospheric plasma-induced surface copolymerization, ACS Appl. Mater. Interfaces 3 (2011) 1228–1237.